scientific reports

Check for updates

OPEN

MiR-363-3p induces tamoxifen resistance in breast cancer cells through PTEN modulation

Yaning Liang[1], Cuiyu Shi[1], Yu Wang[2], Bingjie Fan[3], Wei Song[1] & Rong Shen[1]✉

Nowadays, the investigation for overcoming tamoxifen (TAM) resistance is confronting a considerable challenge. Therefore, immediate attention is required to elucidate the mechanism underlying TAM resistance in breast cancer. This research primarily aimed to define how miRNA-363-3p facilitates resistance to TAM in breast cancer. High-throughput miRNA sequencing was performed using RNAs prepared from breast cancer MCF-7 cells and TAM-resistant MCF-7 cells (MCF-7-TAM). An increase in miRNA-363-3p levels was observed in MCF-7-TAM cells. In MCF-7 cells, miRNA-363-3p directly targeted and negatively regulated phosphatase and tensin homolog (PTEN). Reduction of miRNA-363-3p retarded cell growth and accelerated cell apoptosis, thereby enhancing the sensitivity of TAM. Moreover, analysis using the Kyoto Encyclopedia of Genes and Genomes (KEGG) pathway showed significant enrichment of target genes within the phosphoinositide-3-kinase (PI3K)/protein kinase B (AKT) signaling pathway. Ultimately, miR-363-3p decreased the responsiveness of breast cancer cells to TAM by targeting and suppressing PTEN through a mechanism associated with the PI3K-Akt pathway. Therefore, these results suggest that miR-363-3p-dependent PTEN expression contributes to the mechanisms underlying breast cancer endocrine resistance.

Keywords Hsa-miR-363-3p, Breast cancer, PTEN, TAM resistance, PI3K/AKT signaling pathway

Breast cancer is the most prevalently diagnosed cancer in women[1], which leads the greatest number of cancer-related fatalities among women over 45. Its morbidity and mortality are anticipated to rise significantly over the subsequent 5 to 10 years, reflecting the sluggish advancement in the prevention and treatment of this disease[2,3]. The majority of breast cancer cases are estrogen receptor (ER) positive, which is associated with the highest mortality rates among breast cancer patients[4]. Tamoxifen (TAM) is the primary treatment for this type of breast cancer. It suppresses tumor cell growth by competitively binding to ER, forming a stable complex that effectively impedes DNA replication in the nucleus and playing a significant role in averting contralateral breast cancer. A 5-year regimen of TAM has been shown to reduce breast cancer mortality by over one-third within the first 15 years. However, some patients with ER-positive early breast cancer develop novel or acquired drug resistance, resulting in tumor recurrence and metastasis[5]. Therefore, exploring the mechanisms underlying TAM resistance in breast cancer is of paramount significance.

MicroRNAs (miRNAs), a class of short non-coding RNAs, could modulate mRNA expression either by targeting their 3′ non-coding regions or by promoting their degradation[6]. miRNAs have been demonstrated to bo involved in tumorigenesis, metastasis, and drug resistance[7]. For instance, miR-29a reversed drug resistance induced by p-glycoprotein and decelerated the growth of colon cancer cells by upregulating phosphatase and tensin homolog (PTEN)[8]. Conversely, activation of the miR-371/372/373 cluster enhanced malignancy and decreased drug sensitivity in oral cancer cells[9]. A study indicated that miR-378a-3p contributes to TAM resistance in breast cancer by modulating GOLT1A[10]. miR-663b modulated breast cancer sensitivity to TAM by mediating tumor protein 73 (TP73) expression[11]. Monopolar spindle 1 promoted breast tumor resistance to TAM by phosphorylating estrogen receptor α[4]. Therefore, it is crucial to investigate whether other miRNAs can mediate TAM resistance and to explore the underlying mechanisms.

miR-363-3p has been found to be aberrantly expressed in several cancers, including liver cancer[12], gastric cancer[13], and glioma[14]. It belongs to the miR-106a-363 cluster[15], which is a paralog of miR-17-92, a well-known oncogenic cluster[16]. Notably, previous studies have revealed that miR-363-3p promotes the progression of

[1]Department of Minimally Invasive Oncology, Shandong Provincial Hospital Affiliated to Shandong First Medical University, Jinan 250021, Shandong, China. [2]Tumor Research and Therapy Center, Shandong Provincial Hospital Affiliated to Shandong First Medical University, Jinan 250021, Shandong, China. [3]Cancer Research Center, Shandong Cancer Hospital and Institute, Shandong First Medical University, Shandong Academy of Medical Sciences, Jinan 250117, Shandong, China. ✉email: shenrong20@126.com

prostate cancer via Dickkopf-3 and suppresses the malignancy of non-small cell lung cancer cells via neural progenitor cell expression as well as development 9 (NEDD9) and SOX4[17,18]. Additionally, it shows significant downregulation in osteosarcoma tissues in contrast to adjacent non-cancerous tissues, restraining the growth as well as invasion of osteosarcoma cells through its interaction with SOX4[19]. Furthermore, the interaction between miR-363-3p as well as the long non-coding RNA XIST was observed to enhance the accelerated growth of lung adenocarcinoma cells by upregulating murine double minute 2 (MDM2), a key regulator of the anti-oncogene p53[20]. These findings jointly emphasize the importance of miR-363-3p in various types of cancer. Thus, this research was designed to clarify the biological function of miR-363-3p and its underlying mechanisms in breast cancer, particularly regarding TAM resistance.

Materials and methods

Cells and main reagents

The MCF-7 human breast cancer cell line was procured from the Shanghai Biobank, Chinese Academy of Sciences. We procured miR-363-3p mimics along with their control (miR-NC), as well as the miR-363-3p knockdown plasmid (si-miR-363-3p) and its corresponding control (si-NC) from Biotech (Shanghai). The ultra-pure RNA extraction kit, SYBR Green Pro Taq HS premix qPCR kit, and Evo M-MLV reverse transcription reagent premix were procured from Acres Biologicals. The dual luciferase reporter system was acquired from Promega. The Cell Counting Kit-8 (CCK-8) was obtained from Wuhan Xavier Biotechnology Co. Antibodies targeting P-AKT, PI3K, PTEN, and caspase-3 were purchased from Proteintech, whereas those against P-PI3K, GAPDH, and Ki67 were sourced from ABclonal. The HRP-labeled goat anti-rabbit secondary antibody was procured from Nakasugi Jinqiao.

Cell culture

MCF-7 cells were cultured in Dulbecco's Modified Eagle's Medium supplemented with 10% fetal bovine serum, 100 U/mL penicillin, and 100 μg/mL streptomycin at 37 °C in a 5% CO_2 atmosphere. Experiments were carried out using cells during their logarithmic growth phase. Low-concentration induction method was utilized to construct TAM-resistant MCF-7 cells lines (MCF-7-TAM)[21]. Briefly, MCF-7-TAM cells were generated by gradually increasing the dose of 4-hydroxyTAM in culture from 10 nM to 10 μM, allowing for stable growth in a growth medium containing 10 μM TAM. Lipofectamine 2000 was applied for the transfection of miR-NC, miR-363-3p mimics, si-NC, as well as si-miR-363-3p into both MCF-7 and MCF-7-TAM cells, resulting in the creation of the miR-NC, OE-miR-363-3p, si-NC, and si-miR-363-3p groups, respectively. Untreated cells were employed as the control group. Cell collection took place 48 h post-transfection to assess the transfection effects utilizing real-time fluorescence quantitative polymerase chain reaction (RT-qPCR).

RNA extraction and high-throughput sequencing

Total RNA was extracted from MCF-7 and MCF-7-TAM cells utilizing the ISOGEN reagent following the manufacturer's instructions. Small RNA cDNA library was carried out from the total RNAs and high-throughput sequencing was conducted using an Illumina GAIIx sequencer[22]. The clean reads from small RNA (sRNA) sequencing were first mapped onto the reference genome using comparative analysis software to ensure the quality of the sequencing data. Subsequently, miRNAs were identified, their expression was analyzed and sRNA sequences from each sample were compared with the sequences of the specified species in the miRBase database to screen for differentially expressed miRNAs. The $\log_2$ (transcripts per million) values for each sample were calculated and clustered. Target genes were predicted for the known and novel miRNAs which were differentially expressed. Gene ontology (GO) analysis and Kyoto Encyclopedia of Genes and Genomes (KEGG) pathway analysis were performed to analyze the differentially expressed genes (DEGs). $P < 0{\cdot}05$ was set as the significant criterion and the results were visualized using the ggplot2 package.

RT-qPCR

We isolated total RNA using TRIzol reagent. The cDNAs were reverse transcribed from the isolated RNAs by assembling the following reaction on ice: 2 μL of 5 × Evo M-MLV RT Master Mix, 500 ng of total RNA and 10 μL of RNase-free water. RT-qPCR was carried out using SYBR Green Premix and specific PCR primers. The internal reference gene employed was U6. The primer sequences utilized were as follows: hsa-miR-363-3p-F: 5′-CCAATTGCACGGTATCCATCT-3′, hsa-miR-363-3p-R: 5′-ATCCAGTGCAGGGTCCGAGG-3′, hsa-miR-363-3p-RT: 5′-GTCGTATCCAGTGCAGGGTCCGAGGTATTCGCACTGGATACGACTACAGA-3′; hsa-miR-155-5p-F: 5′-CCCCGTTAATGCTAATCGTGATAG-3′, hsa-miR-155-5p-R: 5′-ATCCAGTGCAGGGTCCGAGG-3′, hsa-miR-155-5p-RT: 5′-GTCGTATCCAGTGCAGGGTCCGAGGTATTCGCACTGGATACGACAACCCC-3′; hsa-miR-148a-3p-F: 5′-CTCAGTGCACTACAGAACTTTGT-3′, hsa-miR-148a-3p-R: 5′-ATCCAGTGCAGGGTCCGAGG-3′, hsa-miR-148a-3p-RT: 5′-GTCGTATCCAGTGCAGGGTCCGAGGTATTCGCACTGGATACGACACACAAAG-3′; U6-F: 5′-GCTCGCTTCGGCAGCACA-3′, U6-R: 5′-GAACGCTTCACGAATTTGCGTG-3′.

Western blotting

Cell lysis was carried out using 200 μL of radioimmunoprecipitation assay buffer. The lysates were centrifuged at high speed at 4 ℃. Protein quantification in the supernatants was conducted using a specialized kit, and subsequently separated by SDS-PAGE. The protein was transferred onto a PVDF membrane and subsequentlyincubated with overnight at 4 ℃ using primary antibodies (AKT, 1:5000; p-AKT and PTEN, 1:10,000; PI3K, 1:500; p-PI3K, 1:1000; GAPDH, 1:5000) and maintained with HRP-labeled secondary antibody (1:10,000). Equal volumes of enhanced chemiluminescence A and B reagents were mixed in a dark room, and the membranes were immersed in the mixture for 5 min. The residual liquid in the upper layer was aspirated

prior to exposing the membranes for processing. The grayscale values of the target bands were determined, and the expression levels were obtained with respect to the internal reference.

CCK-8 assay

A 100 µL aliquot of MCF-7-TAM cell suspension was added to each well. In accordance with the experimental grouping, cells were treated with 5 µM of the drug, ensuring that volume of the drug did not exceed one-tenth of the volume of the cell suspension. Finally, after incubation with 10 µL of CCK-8 reagent for 4 h, the optical density of the cells at 450 nm was determined using a microplate reader.

Colony formation assay

Cells were seeded in 6-well plates at a density of 1000 cells per well and incubated them for 2 weeks. The cells were fixed with 1 mL of 4% paraformaldehyde and subsequently stained with 500 µL of crystal violet solution for 20 min. Finally, the colonies were photographed for enumeration.

Immunocytochemistry and fluorescence imaging

MCF-7 and MCF-7-TAM cells were fixed for 20 min at 4 ℃ with 4% paraformaldehyde in phosphate-buffered saline (PBS), and then the immunostaining process was carried out. For the immunostaining process, after blocking with 5% normal goat serum and 1% bovine serum albumin in PBS at room temperature for 1 h, the coverslips or slides were incubated with primary antibodies at 4 ℃ overnight and then with secondary antibodies at room temperature for 60–90 min. Following several washes with PBS, cells or slides were mounted with Vectashield with DAPI. Fluorescence images were acquired with Olympus FluoView and Leica TCS SP8 laser scanning confocal microscope.

The counting of positive cells was carried out using ImageJ software. The fluorescence image was converted into 8-bit format for threshold segmentation. Select "Image"→"Adjust"→"Threshold", and a shreshold adjustment dialog box will pop up. By dragging the slider, the positive signal wsa distinguished from the background. Click "Apply". Subsequently, the particle analysis operation was performed to identify the number of positive cells and record it in the experimental data table for subsequent statistical analysis. To visually display the relative expression levels of Ki-67/caspase 3, the ratios of Ki-67/caspase 3 positive cells were normalized based on the MCF-7-TAM group and visualized in the form of a histogram.

Dual luciferase reporter assay

TargetScan was employed to predict the 3′-untranslated region (3′-UTR) of PTEN contains complementary sequences. Wild-type (WT) or mutant (MT) 3′-UTR sequences of PTEN, containing the miR-363-3p binding site, were inserted into the luciferase reporter plasmid to generate the luciferase reporter vector. The WT-PTEN or MT-PTEN reporter vector was co-transfected with either the miR-363-3p or miR-NC expression plasmid into the cells and incubated for 48 h. Then the cell lysis was carried out using a passive lysis buffer. The background absorbance was ascertained using 20 µL of cell lysis buffer. We added a 20 µL working solution of Luciferase Assay Reagent II to each well and then measured the absorbance. Finally, 20 µL of Stop & Glo® Reagent was added to each well, followed by measuring the absorbance.

Statistical analysis

We conducted statistical analysis utilizing SPSS 21.0 software and generated graphs using GraphPad Prism 9.0. Each experiment was repeated three times. Data were presented as the mean ± standard deviation. Dunnett's t-test was utilized to compare between two experimental groups, while one-way analysis of variance (ANOVA) was employed for comparisons involving multiple groups of data. The least significant difference test was carried out, and the difference was significant when P value < 0.05.

Results

Differential miRNA expression between MCF-7 as well as MCF-7-TAM cells

Identification of miRNAs differentially expressed in MCF-7 and MCF-7-TAM cells

As depicted in Fig. 1A, the results of colony formation experiments and CCK-8 experiments confirm the successful establishment of MCF-7-TAM. We mapped all clean reads to the genomic reference sequence (Fig. 1B) and found that more than 80% of the clean reads corresponded to the reference genome (one mismatch allowed). This instilled confidence in the subsequent analysis results. Subsequently, every unique sRNA read was annotated (Table 1). The results demonstrated that this high-throughput sequencing sample was of good quality.

The overall distribution of differentially expressed miRNAs was visualized using volcano plots. In contrast to MCF-7 cells, MCF-7-TAM cells had 178 upregulated as well as 169 downregulated miRNAs (Fig. 1C). $P < 0.05$ as well as $|\log_2 (\text{fold\_change})| \geq 1$ was applied to identify differentially expressed miRNAs. Meanwhile, clustering analysis was carried out on miRNAs to explore the co-expression patterns of miRNA (Fig. 1D). The expression profile revealed that there were obviously enriched some differentially expressed genes between MCF-7 and MCF-7-TAM cells.

RT-qPCR validation

From the 347 differentially expressed miRNAs identified, RT-qPCR was carried out on the two with the smallest p-values and the three with the greatest fold change to verify whether miR-363-3p was upregulated in MCF-7-TAM cells (Fig. 1E; Table 2). We observed miR-363-3p to be obviously highly expressed in MCF-7-TAM cells as well as significantly lowly expressed in MCF-7 cells ($P < 0.05$).

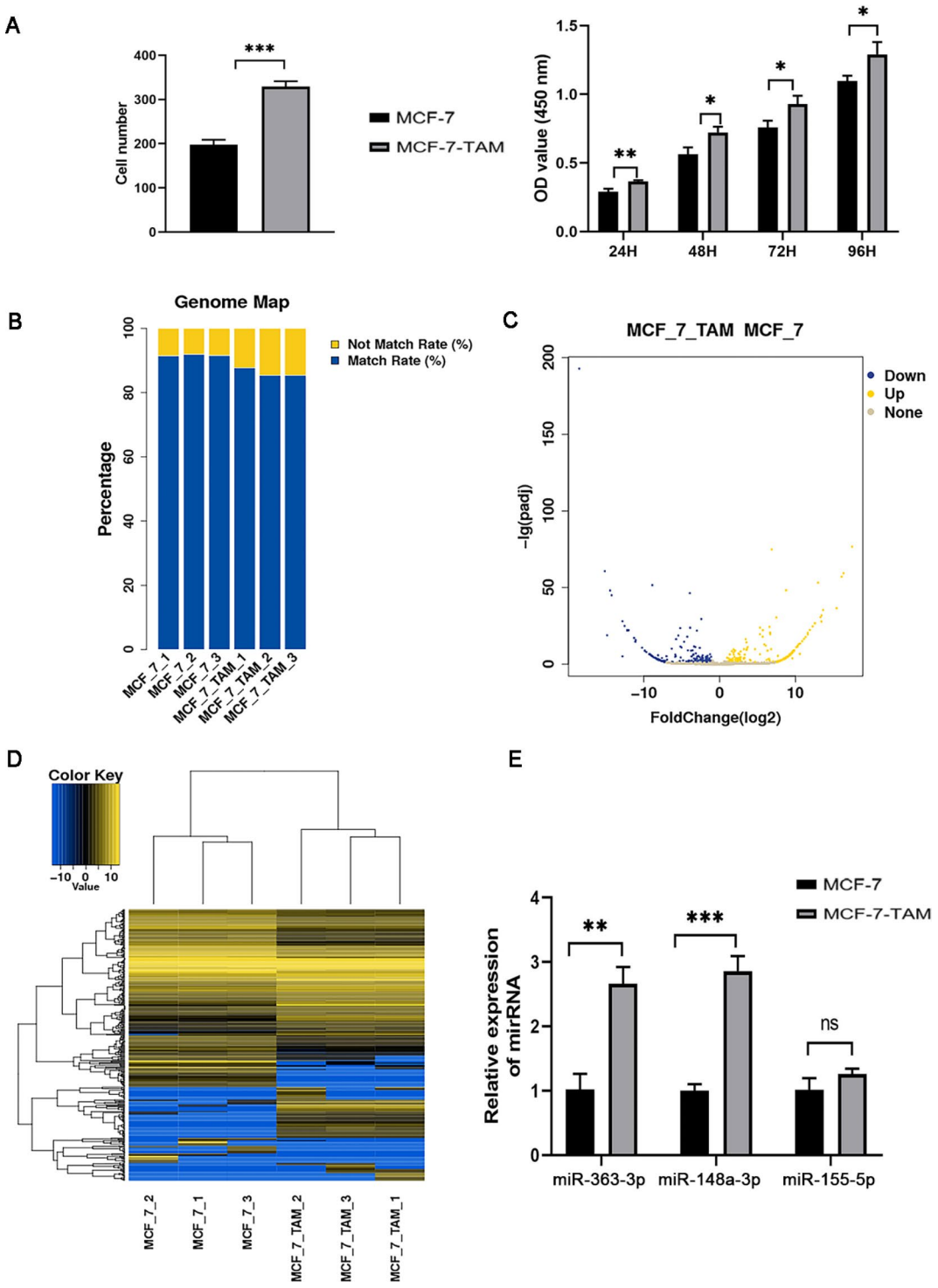

Fig. 1. Differential miRNA expression between MCF-7 as well as MCF-7-TAM cells. (**A**) Colony formation assay and CCK-8 assay. (**B**) Comparison rate analysis chart. Match rate (%): the percentage of clean reads that matched with the genomic reference sequence (one mismatch allowed); Non-match rate (%): the percentage of clean reads that did not match with the genomic reference sequence (greater than one mismatch). (**C**) Volcano plot of variance analysis results. The horizontal coordinates represent ploidy changes in miRNA expression in different experimental groups/samples. The vertical axis represent the statistical significance of changes in miRNA expression. The scattered dots represent individual miRNAs, the gray dots indicate miRNAs that are not significantly differentially expressed, the yellow dots indicate significantly upregulated miRNAs and the blue dots indicate significantly downregulated miRNAs. (**D**) Differential miRNA clustering analysis. Columns indicate different samples, rows indicate different genes, yellow represents upregulated genes and blue represents downregulated genes. (**E**) The overexpression of miR-363-3p in MCF-7-TAM cells was verified by RT-qPCR. $^{*}P < 0.05$, $^{**}P < 0.01$; $^{***}P < 0.001$. TAM, tamoxifen; RT-qPCR, real-time fluorescence quantitative polymerase chain reaction.

Types	MCF_7_1	MCF_7_2	MCF_7_3	MCF_7_TAM_1	MCF_7_TAM_2	MCF_7_TAM_3
Total	100.00	100.00	100.00	100.00	100.00	100.00
known_miRNA	14.23	12.91	20.32	32.76	38.84	33.95
rRNA	54.57	57.25	49.15	19.61	16.76	22.58
tRNA	1.78	1.83	2.20	2.41	1.97	2.62
snRNA	0.30	0.28	0.23	0.13	0.12	0.13
snoRNA	1.42	1.35	1.08	1.14	1.63	1.69
other_rfam	3.91	3.92	3.22	8.02	7.38	7.05
Repeat	0.85	0.87	1.08	2.02	2.65	2.30
exon:+	1.02	1.03	1.36	1.18	1.11	1.17
exon:-	0.07	0.07	0.12	0.28	0.23	0.21
intron:+	0.64	0.52	0.94	1.66	1.39	1.33
intron:-	3.17	3.12	2.86	2.68	2.75	2.62
piRNA	0.00	0.00	0.00	0.00	0.01	0.03
novel_miRNA	0.46	0.79	0.90	2.29	2.56	2.12
Other	17.58	16.06	16.54	25.81	22.60	22.20

Table 1. Statistical table of sRNA classification and their comparison (%). Types: sample name and proportion; total: the number and proportion of reads in each sample; known_miRNA: the number and proportion of sRNAs that align with known miRNAs in each sample; rRNA/tRNA/snRNA/snoRNA/other_rfam: the number and proportion of different types of sRNAs that correspond to entries in the Rfam database in each sample; repeat: the number and proportion of sRNAs that match with repetitive sequences in each sample; exon:+/exon:-/intron:+/intron:-: the number and proportion of positive and negative strands that match with exons/introns in each sample; piRNA: the number and proportion of piRNA that match piRNA Bank in each sample; novel_miRNA: the number and proportion of sRNAs annotated as novel miRNAs in each sample; other: the number and proportion of sRNAs that match reference sequences but do not belong to known miRNAs, ncRNAs, repeat regions, exons, introns and novel miRNAs in each sample. sRNA, small RNA; miRNA, micro RNA; ncRNA, non-coding RNA.

Gene name	Fold change	pval
hsa-miR-148a-3p	118.56	1.84E–78
hsa-miR-363-3p	8224.02	2.03E–56
hsa-miR-9-5p	438.85	2.56E–51
hsa-miR-155-5p	44903.53	1.8E–39
hsa-miR-455-5p	11041.31	1.49E–30

Table 2. Differentially expressed miRNAs (lowest pval). Fold Change: Fold change in the mean expression between the experimental and control groups; pval: p-value, a smaller p-value indicates a larger fold difference.

GO and KEGG enrichment analysis

GO analysis facilitates the understanding the biological processes, molecular functions, and cellular components associated with the gene sets, while KEGG analysis provides insights into the metabolic pathways and regulatory networks in which these genes are implicated. In Fig. 2A, GO enrichment analysis revealed that genes targeted by differentially expressed miRNAs in MCF-7-TAM cells were mainly involved in biological processes such as bioregulation and metabolism, cellular components like organelles, cell membranes and other components and molecular functions like binding and catalysis. As Fig. 2B shown, the target genes exhibited notable enrichment primarily within the PI3K–Akt signaling pathway, and the regulation of actin cytoskeleton, cAMP signaling pathway, as well as spinocerebellar ataxia.

Inhibition of mir-363-3p increased the sensitivity of MCF-7-TAM cells to TAM

Effects of Mir-363-3p downregulation on cell proliferation

To investigate the impact of miR-363-3p on the response of breast tumors to TAM, we knocked down miR-363-3p in MCF-7-TAM cells. Figure 3A implied that the cells were successfully transfected ($P<0.05$). The proliferative capacity of tumor cells was evaluated by the CCK-8 (Fig. 3B) and colony formation assay (Fig. 3C). Cell proliferation and colony formation were significantly attenuated in the MCF-7-TAM-si-miR-363-3p group in comparison with the MCF-7-TAM-NC cells ($P<0.05$). Moreover, inhibition of miR-363-3p combined with TAM treatment notably impeded the proliferation and colony formation ability of MCF-7-TAM cells ($P<0.05$).

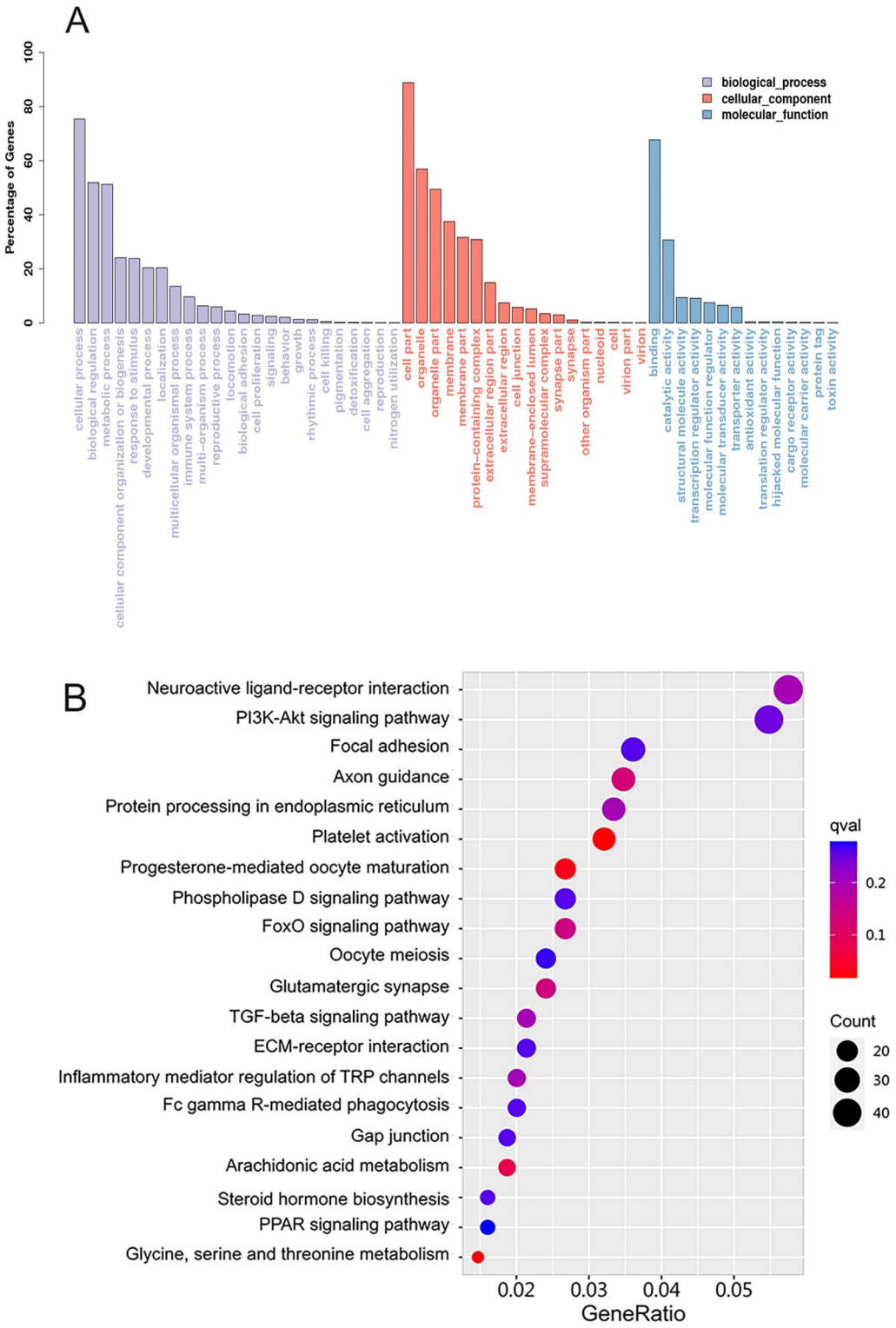

Fig. 2. GO and KEGG enrichment analysis. (**A**) Bar graph depiction of the GO enrichment analysis of the target genes of differentially expressed miRNAs. GO, Gene Ontology. The different colors signify the three broad categories of GO enrichment: biological processes, cellular components and molecular function. (**B**) KEGG enrichment analysis. KEGG, Kyoto Encyclopedia of Genes and Genomes. The size of each dot indicates the number of genes enriched in that GO subcategory. Larger dots indicate more genes enriched in that GO subcategory and vice versa.

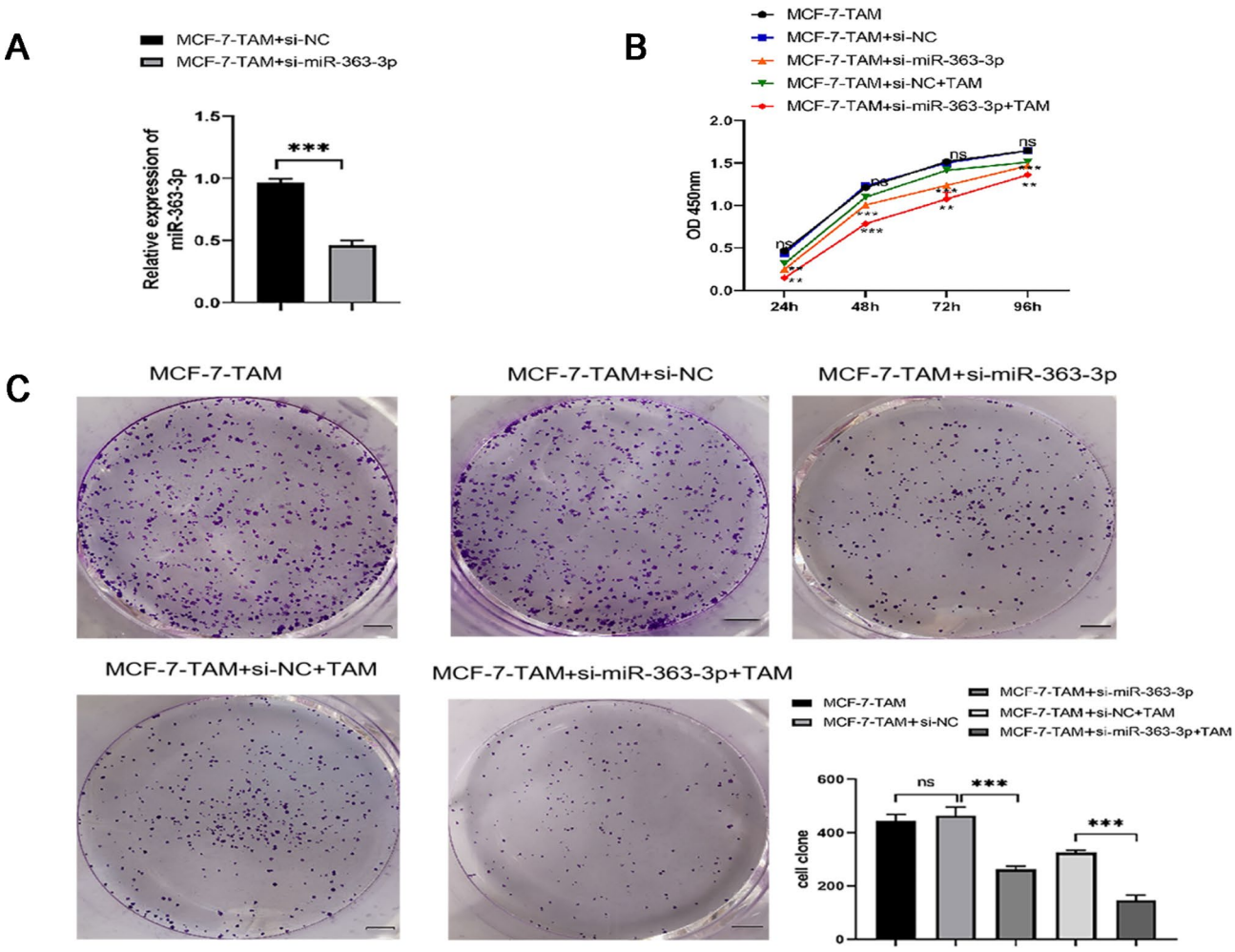

Fig. 3. Alterations in cell proliferation after downregulating miR-363-3p. (**A**) Validation of successful transfection targeting miR-363-3p via RT-qPCR. (**B**) Alterations in cell proliferation subsequent to the knockdown of miR-363-3p and treatment with TAM. (**C**) Alterations in the number of colonies formed of treatment with si-miR-363-3p as well as TAM. $^{**}P < 0.01$; $^{***}P < 0.001$. Scale bar: 3 mm.

These results suggested that inhibiting miR-363-3p reduced resistance and enhanced cell sensitivity to TAM in MCF-7-TAM cells.

Effects of Mir-363-3p downregulation on cell proliferation as well as apoptosis markers

To confirm the aforementioned results, we examined the effects of downregulating miR-363-3p on the cell proliferation marker Ki-67 (Fig. 4A) and the apoptosis marker caspase-3 (Fig. 4B) using immunocytochemistry and fluorescence imaging. The count of Ki-67 positive cells was markedly decreased while that of caspase-3 positive cells was increased in miR-363-3p-inhibited MCF-7-TAM cells. These markers displayed a similar expression pattern in miR-363-3p-inhibited MCF-7-TAM cells treated with TAM. Consequently, inhibiting miR-363-3p could reduce TAM resistance in TAM-resistant breast cancer cells, enhancing the toxic effect of TAM on these cells.

Overexpression of mir-363-3p increased the resistance of breast cancer cells to TAM

Function of mir-363-3p upregulation on cell growth

miR-363-3p mimics were applied to transfect MCF-7 cells, and RT-qPCR experiment demonstrated the successful transfection ($P < 0.001$; Fig. 5A). The proliferation and colony formation abilities of miR-363-3p-overexpressing MCF-7 cells were significantly enhanced with those of MCF-7-NC cells ($P < 0.001$; Fig. 5B,C). Similarly, the proliferation and colony formation abilities of miR-363-3p-overexpressing MCF-7 cells treated with TAM were remarkably higher than those of MCF-7-NC cells treated with TAM ($P < 0.05$; Fig. 5B,C). These results suggested that miR-363-3p upregulation decreased breast cancer cell sensitivity to TAM.

Impacts of mir-363-3p upregulation on cell proliferation and apoptosis markers

For further verification of the impact of miR-363-3p overexpression on the sensitivity of breast cancer cells to TAM, we examined alterations in the expression levels of Ki-67 (Fig. 6A) and caspase-3 (Fig. 6B). The

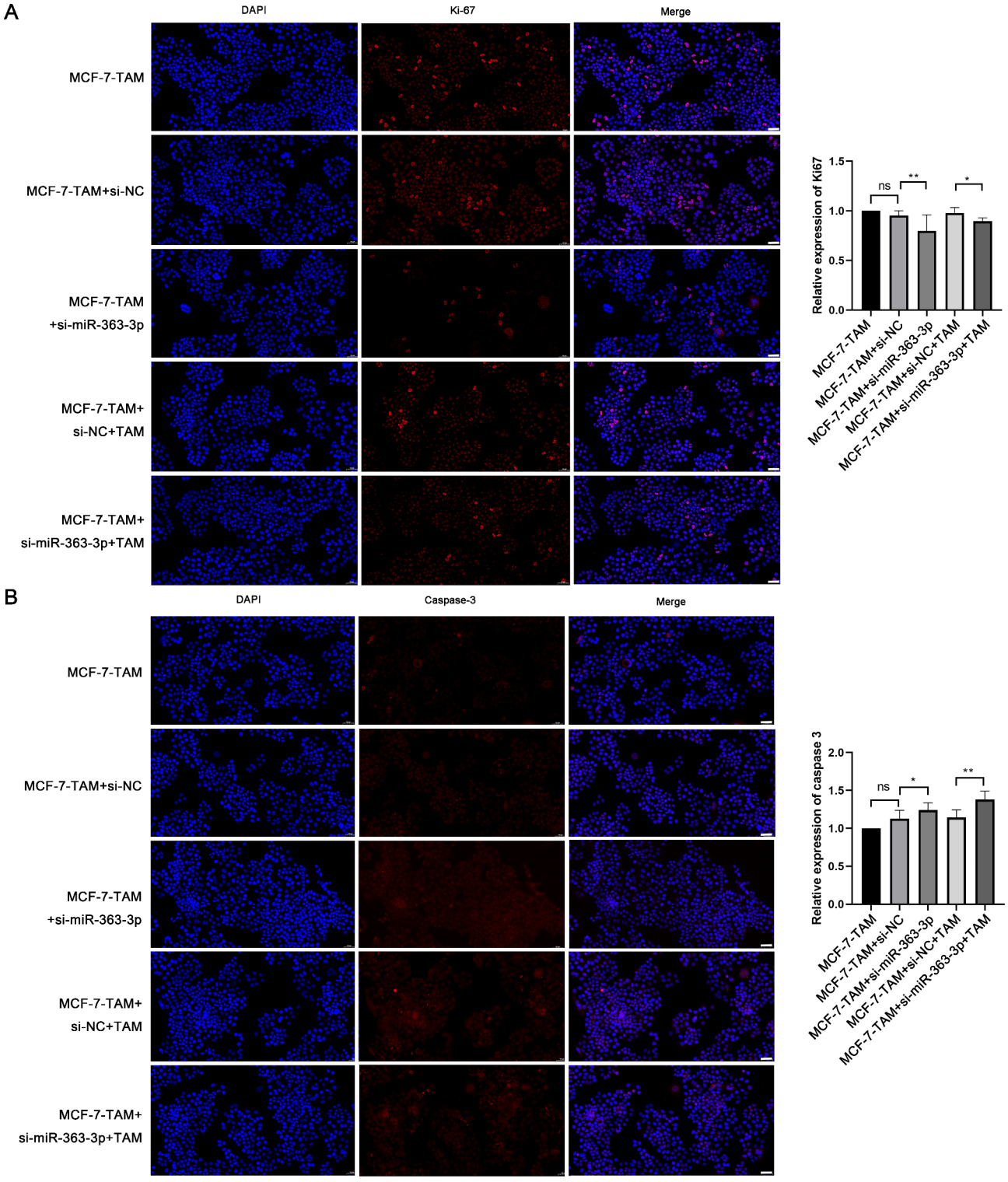

Fig. 4. Impacts of the knockdown of miR-363-3p on cell proliferation and apoptosis. The alterations in the cell proliferation marker Ki-67 (A) and the apoptosis marker caspase-3 (B) subsequent to the knockdown of miR-363-3p and the treatment of TAM were examined via immunofluorescence (IF). $^{*}P < 0.05$, $^{**}P < 0.01$, $^{***}P < 0.001$. Scale bar: 50 μM.

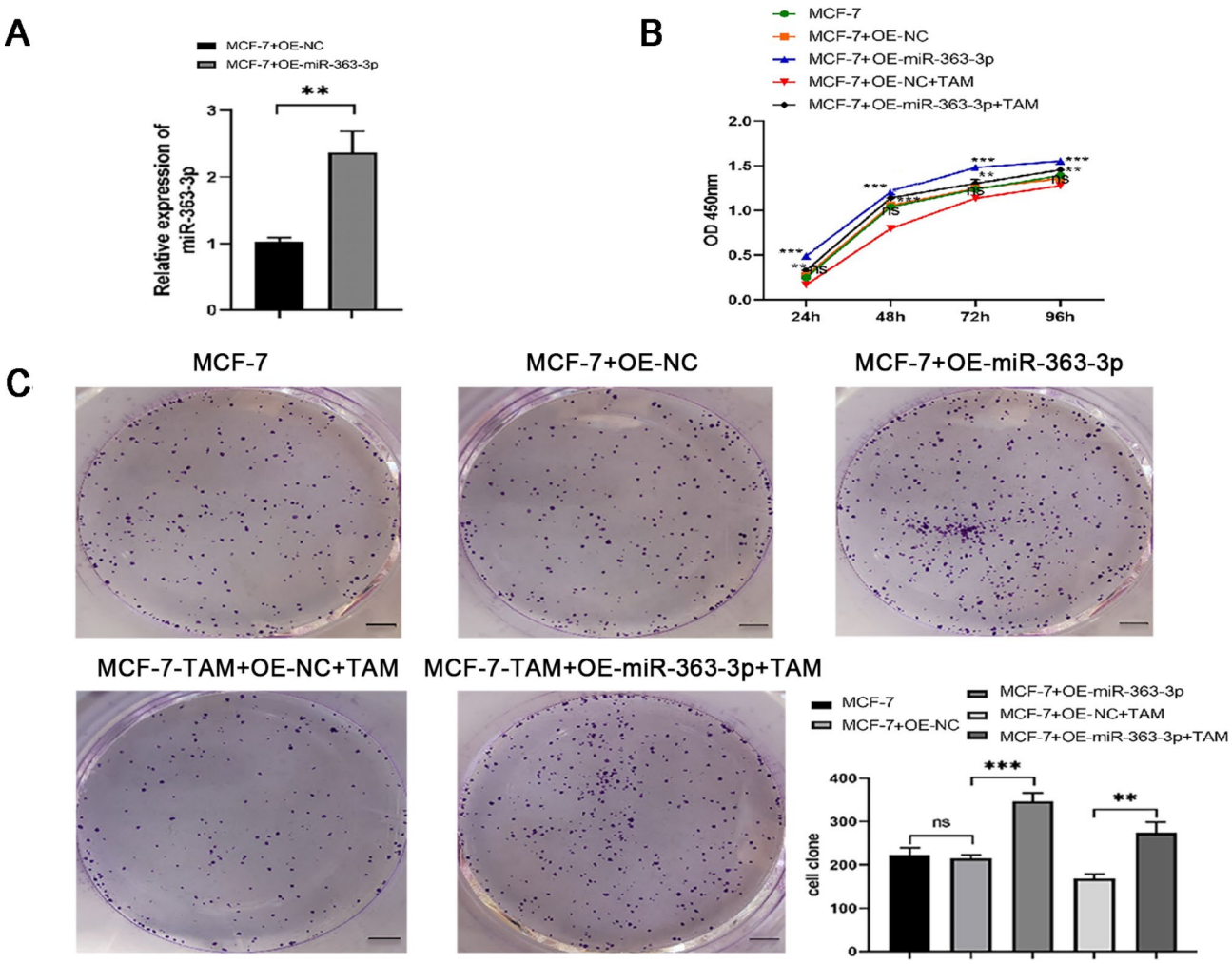

Fig. 5. Alterations in cell proliferation after miR-363-3p upregulation. (**A**) Verification of successful transfection for overexpressing miR-363-3p. (**B**) Alterations in cell proliferation. (**C**) Changes in the colony formation ability. $^{**}P < 0.01$; $^{***}P < 0.001$. Scale bar: 3 mm.

count of Ki-67 positive cells was significantly increased while that of caspase-3 positive cells reduced in MCF-7 cells overexpressing miR-363-3p. We noted a comparable expression pattern in TAM-treated miR-363-3p-overexpressing MCF-7 cells compared with TAM-treated MCF-7-NC cells. These results indicated that upregulating miR-363-3p increased the resistance of breast cancer cells to TAM, attenuating the toxic effects of the drug on these cells.

Mir-363-3p promoted PI3K–AKT signaling pathway by inhibiting PTEN in breast cancer cells

PTEN was a target of mir-363-3p in breast cancer cells

We screened potential gene targets of miR-363-3p via miRanda. GO enrichment and KEGG pathway analysis revealed that the PI3K–AKT pathway was relatively significantly enriched with these gene targets (Fig. 2B). Since PTEN was an important regulator of this pathway, we investigated it as a candidate gene target for miR-363-3p using dual luciferase reporter experiments. The WT as well as a MT 3′-UTR of PTEN, which contains the probable miR-363-3p binding site, were cloned into the luciferase reporter vector psi-CHECK2 (Fig. 7A). miR-363-3p significantly attenuated the luciferase activity in MCF-7 cells transfected with the WT reporter vector but not the MT reporter vector ($P < 0.05$; Fig. 7A). This experiment demonstrated that miR-363-3p specifically bound to a particular site in the 3′-UTR of PTEN.

Mir-363-3p inhibited PTEN level in breast cancer cells

Further, to elucidate the regulatory association between miR-363-3p and PTEN, PTEN expression was examined in MCF-7 cells, MCF-7-TAM cells, miR-363-3p-overexpressing MCF-7 cells and miR-363-3p-inhibited MCF-7-TAM cells (Fig. 7B). In comparison with MCF-7 cells, PTEN was significantly downregulated in MCF-7-TAM cells ($P < 0.05$). Similarly, in comparison with the MCF-7-NC group, PTEN expression was notably decreased in MCF-7 cells overexpressing miR-363-3p ($P < 0.05$). Conversely, in comparison to the MCF-7-TAM-NC group, inhibiting miR-363-3p in MCF-7-TAM cells evidently enhanced PTEN expression ($P < 0.05$). These results

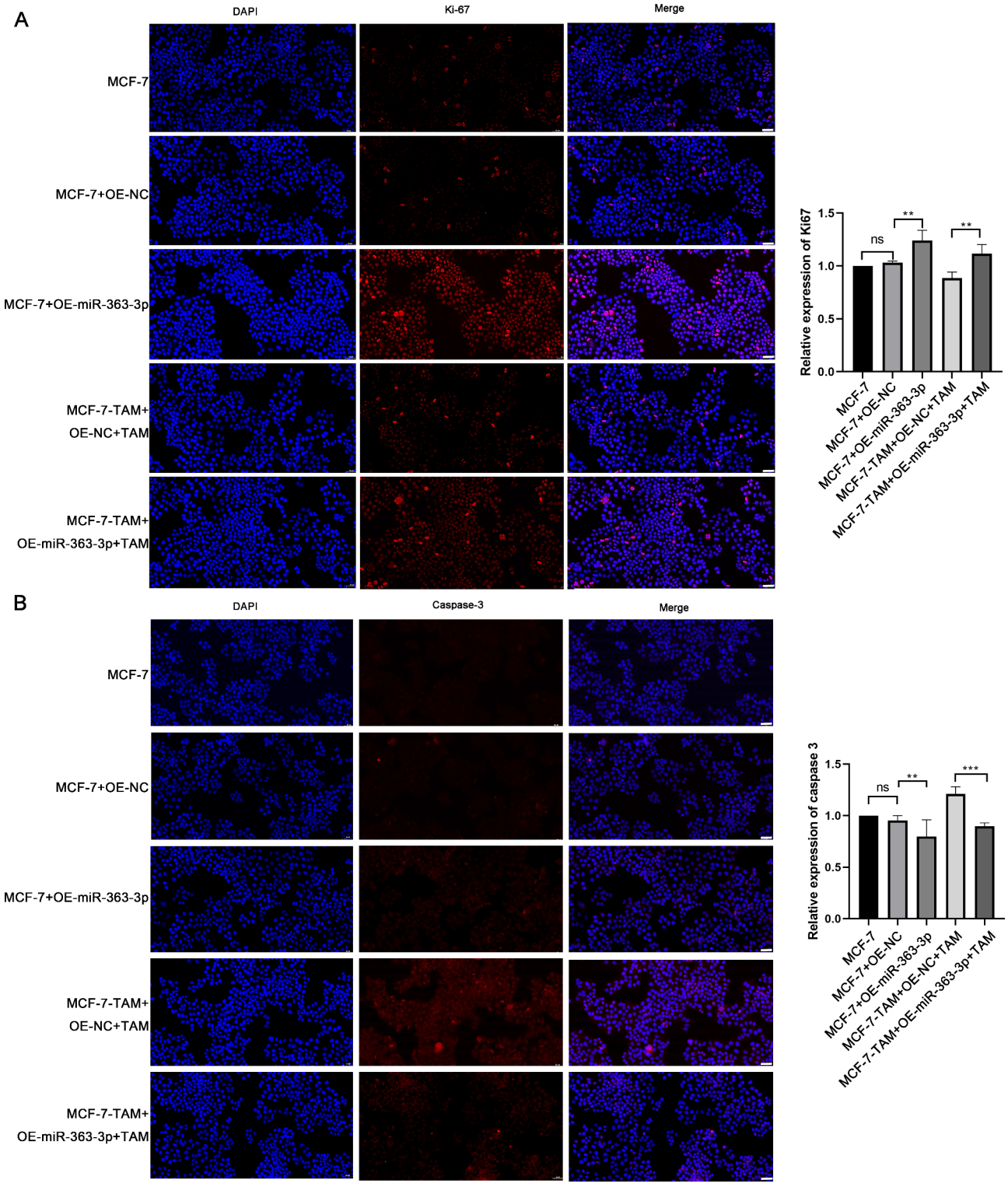

Fig. 6. Impacts of the overexpression of miR-363-3p on cell proliferation and apoptosis. The alterations in the cell proliferation marker Ki-67 (A) and the apoptosis marker caspase-3 (B) subsequent to the overexpression of miR-363-3p and the treatment of TAM were examined via IF. $^{**}P < 0.01$, $^{***}P < 0.001$. Scale bar: 50 μm.

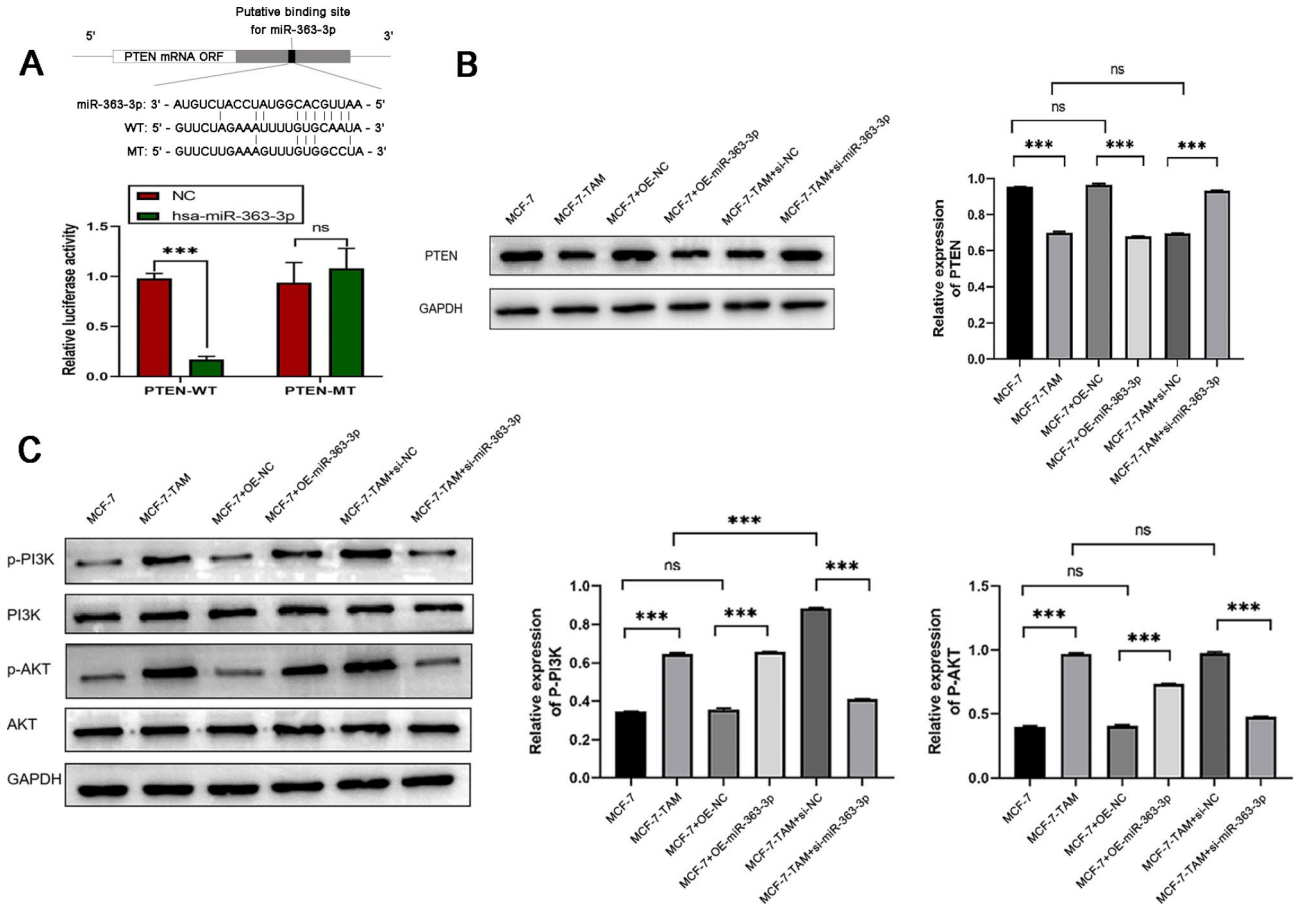

Fig. 7. miR-363-3p promoted PI3K–AKT signaling by inhibiting PTEN in breast cancer cells. (**A**) Dual luciferase assay verified that PTEN was a gene target of miR-363-3p. (**B**) PTEN protein expression in breast cancer cells was detected by Western blotting. (**C**) The expression of proteins related to the PI3K–AKT pathway was detected in breast cancer cells by Western blotting. $^{***}P < 0.001$. PI3K, phosphoinositide 3-kinase.

revealed that overexpressing miR-363-3p decreased PTEN level in TAM-sensitive breast cancer cells, whereas inhibiting of miR-363-3p increased PTEN level in TAM-resistant cancer cells, demonstrating the negative regulatory effect of miR-363-3p on PTEN.

Mir-363-3p promoted PI3K–AKT signaling pathway by inhibiting PTEN in breast cancer cells

We hypothesized that miR-363-3p overexpression as well as inhibition may affect PI3K–AKT signaling pathway in breast cancer cells. RNA sequencing as well as RT-qPCR demonstrated that miR-363-3p level was notably increased in MCF-7-TAM cells in comparison with MCF-7 cells. Furthermore, PI3K as well as AKT protein levels were obviously augmented in MCF-7-TAM cells compared with MCF-7 cells as well as in MCF-7 cells overexpressing miR-363-3p in contrast to MCF-7-NC cells ($P < 0.05$; Fig. 7C). Meanwhile, PI3K as well as AKT protein levels were significantly decreased in miR-363-3p-inhibited MCF-7-TAM cells in contrast to MCF-7-TAM-si-NC cells ($P < 0.05$; Fig. 7C). Based on these results, together with those from the CCK-8, colony formation and immunocytochemical staining assays, we concluded that the elevated miR-363-3p level downregulated PTEN and increased PI3K–AKT activity, thus inhibiting apoptosis and enhancing cell proliferation. Conversely, miR-363-3p inhibition increased PTEN expression and suppressed PI3K–AKT signaling, thus promoting apoptosis and reducing cell proliferation. These data indicated that miR-363-3p exerted drug-resistant effects in TAM-resistant breast cancer cells by inhibiting PTEN as well as activating PI3K–AKT signaling.

Discussion

Estrogen-dependent breast cancer comprise more than 70% of all breast cancer cases, and endocrine therapy represents the primary treatment modality for ER-positive patients[23,24]. The most commonly used drugs include TAM, an estrogen blocker, and aromatase inhibitors such as letrozole, anastrozole, and exemestane, which inhibit hormone synthesis in the ovaries[25]. TAM competes with estradiol to bind to ERα, thereby impeding the formation of the ERα-mediated transcriptional complex and suppresses tumor cell proliferation induced by estradiol[26]. Unfortunately, TAM resistance emerges in approximately 20–30% of the cases[27], leading to cancer progression, which eventually seriously threatens the longevity and quality of patients' lives. TAM resistance can manifest before treatment (known as ab initio resistance) or develop during treatment (referred to as acquired

resistance)[28]. The ability to predict resistance phenotypes using biomarkers and the development of alternative treatment regimens can assist in averting the failure of TAM anti-estrogen therapy, making it particularly important to study the mechanisms of resistance and aberrant signaling in breast cancer.

Several miRNAs have been demonstrated to play significant roles in mediating breast cancer resistance to TAM[29–32], including miR-489[33], miR-155[34], miR-186-3p[35], and miR-137[36]. Meanwhile, miR-363-3p was found to be associated with cell proliferation, growth and apoptosis in hepatocellular carcinoma, glioma as well as colorectal cancer (CRC). Wang et al.'s research revealed that miR-363-3p was significantly downregulated in hepatocellular carcinoma (HCC) cells and and its overexpression repressed HCC progression[12]. Downregulation of miR-363-3p in colorectal cancer (CRC) tissues was also detected, with a strong correlation between low miR-363-3p levels and clinical-pathological parameters such as tumor stage and lymph node metastasis[37]. Furthermore, it was proposed that forkhead box P4 protein (FOXP4) overexpression reversed the inhibitory impacts of miR-363-3p mimics on cell proliferation, migration and invasion of gastric cancer cells[13]. HNF1A-AS1 induced the upregulation of MAP2K4 to activate the JNK signaling pathway to promote glioma cell growth by acting as a miR-363-3p sponge[14]. However, the correlation between miR-363-3p as well as breast cancer had not been explored yet. Our study used high-throughput sequencing coupled with RT-qPCR to verify the dysregulation of miR-363-3p in MCF-7-TAM cells compared with MCF-7 cells, implying its involvement in regulating TAM resistance in breast cancer cells. In addition, increasing the expression of miR-363-3p enhanced breast cancer cells' resistance to TAM, while inhibiting miR-363-3p rendered drug-resistant breast cancer cells more sensitive to TAM, indicating that miR-363-3p plays a crucial role in regulating TAM resistance. For future research, further validation in additional cell lines and in vivo models ought to be carried out.

The PTEN gene plays a crucial role in breast cancer biology and functions as a tumor suppressor. Its alterations contribute to cancer aggressiveness by activating pathways like PI3K/AKT, thereby influencing tumor growth and drug resistance. Loss of PTEN function is correlated with poor prognosis and increased recurrence risk in breast cancer patients, rendering it vital for both diagnostic and therapeutic strategies in the management of this disease. The biological effects of PTEN mainly hinge on the ability of its lipid phosphatase motif to dephosphorylate phosphatidylinositol (3,4,5)-trisphosphate (PIP3) at the 3'position to generate PIP2[38]. PI3K, conversely, phosphorylates the hydroxyl group at the third position on the phosphatidylinositol ring of PIP2 to generate PIP3[39]. The accumulation of PIP3 is the main signal for growth factor stimulation. PIP3 was found to recruit downstream proteins to the plasma membrane by binding to their pleckstrin homology domain[40], which enabled their activation via phosphorylation. A well-known downstream effector of PTEN signaling was AKT, which regulated a variety of cellular activities[41]. Loss of PTEN function has been demonstrated to promote aggressive tumor phenotypes by enhancing PI3K-AKT signaling, which is critical for cellular proliferation and survival. This loss is particularly notable in the context of gastric cancer but has significant implications for breast cancer as well, consistent with studies that show concurrent alterations of PTEN and other pathways contribute to poor prognosis[42].

Ongoing research highlights the potential of circulating miRNAs associated with PTEN to serve as biomarkers for treatment response and disease recurrence[43]. Huang et al. have indicated that many miRNAs could directly interact with PTEN mRNA (miR-21, miR-130, miR-214, etc.) or hypomethylate PTEN promoter via DNA methyltransferases (miR-29a, miR-29b, miR-185, etc.) to modify PTEN expression in multiple cancers[44]. Besides, PTEN deletion may be induced by other mechanisms, such as germline and somatic PTEN mutations, genomic deletions, or protein-protein interactions. An in vivo experiment of prostate cancer, PTEN deletion significantly upregulated 16 miRNAs, such as miR-155 and miR-132, and downregulated five miRNAs, including miR-133a and miR-181[45]. Furthermore, miR-26b was found to be abnormally regulated in PTEN-deficient T-cell acute lymphoblastic leukemia in mice[46]. Notably, low PTEN level was detected in ER-positive breast cancer cells as well as correlated with drug resistance in breast cancer patients[47]. miR-301b negatively regulated PTEN, emphasizing its potential as a prognostic biomarker and its importance in the biological processes involved in breast cancer progression[48]. In the current study, to probe into the mechanisms by which miR-363-3p regulated drug resistance in breast cancer cells, we utilized miRanda to predict the candidate targets of miR-363-3p. Further, we noticed that miR-363-3p bound specifically to the WT 3'-UTR of PTEN and notably reduced the luciferase activity of the vector containing it. In contrast, the luciferase vector containing the MT 3'-UTR of PTEN showed higher luciferase activity. These experiments indicated that PTEN was biologically bound to miR-363-3p.

Conclusion

In conclusion, miR-363-3p critically regulates the response of breast cancer cells to TAM and activates the PI3K–AKT pathway by targeting PTEN. Inhibition of miR-363-3p could be a new therapeutic approach to enhance the sensitivity of breast cancer cells to anti-cancer treatment.

Data availability

Data is available on request from the Corresponding author.

Received: 27 March 2024; Accepted: 18 December 2024
Published online: 30 December 2024

References

1. Sung, H. et al. Global Cancer statistics 2020: GLOBOCAN estimates of incidence and mortality worldwide for 36 cancers in 185 countries. *CA Cancer J. Clin.* **71**, 209–249 (2021).
2. Hutchinson, L. Breast cancer: Challenges, controversies, breakthroughs. *Nat. Rev. Clin. Oncol.* **7**, 669–670 (2010).

3. Anastasiadi, Z., Lianos, G. D., Ignatiadou, E., Harissis, H. V. & Mitsis, M. Breast cancer in young women: An overview. *Updates Surg.* **69**, 313–317 (2017).
4. Zhang, X. et al. Monopolar spindle 1 contributes to tamoxifen resistance in breast cancer through phosphorylation of estrogen receptor α. *Breast Cancer Res. Treat.* **202**, 595–606 (2023).
5. Davies, C. et al. Relevance of breast cancer hormone receptors and other factors to the efficacy of adjuvant tamoxifen: Patient-level meta-analysis of randomised trials. *Lancet (London England).* **378**, 771–784 (2011).
6. Bartel, D. P. MicroRNAs: Genomics, biogenesis, mechanism, and function. *Cell* **116**, 281–297 (2004).
7. Vishnoi, A. & Rani, S. MiRNA biogenesis and regulation of diseases: An updated overview. *Methods Mol. Biol. Clifton N J.* **2595**, 1–12 (2023).
8. Shi, X. et al. miRNA-29a reverses P-glycoprotein-mediated drug resistance and inhibits proliferation via up-regulation of PTEN in colon cancer cells. *Eur. J. Pharmacol.* **880**, 173138 (2020).
9. Lin, S. C. et al. Activation of the miR-371/372/373 miRNA cluster enhances oncogenicity and drug resistance in oral carcinoma cells. *Int. J. Mol. Sci.* **21**. (2020).
10. Ikeda, K. et al. miR-378a-3p modulates tamoxifen sensitivity in breast cancer MCF-7 cells through targeting GOLT1A. *Sci. Rep.* **5**, 13170 (2015).
11. Jiang, H., Cheng, L., Hu, P. & Liu, R. MicroRNA–663b mediates TAM resistance in breast cancer by modulating TP73 expression. *Mol. Med. Rep.* **18**, 1120–1126 (2018).
12. Wang, J. et al. LncRNA OIP5-AS1 interacts with mir-363-3p to contribute to hepatocellular carcinoma progression through up-regulation of SOX4. *Gene Ther.* **27**, 495–504 (2019).
13. Ma, H. F., He, W. W. & Wang, J. J. Long noncoding RNA LINC00858 promotes the proliferation, migration and invasion of gastric cancer cells via the miR-363-3p/FOXP4 axis. *Eur. Rev. Med. Pharmacol. Sci.* **24**, 9391–9399 (2020).
14. Bi, Y. et al. Long noncoding RNA HNF1A-AS1 regulates proliferation and apoptosis of glioma through activation of the JNK signaling pathway via miR-363-3p/MAP2K4. *J. Cell. Physiol.* **236**, 1068–1082 (2021).
15. Drobna, M. et al. hsa-miR-20b-5p and hsa-miR-363-3p affect expression of PTEN and BIM tumor suppressor genes and modulate survival of T-ALL cells in vitro. *Cells* 9. (2020).
16. Mavrakis, K. J. et al. Genome-wide RNA-mediated interference screen identifies miR-19 targets in notch-induced T-cell acute lymphoblastic leukaemia. *Nat. Cell. Biol.* **12**, 372–379 (2010).
17. Xu, L. Z., Ning, J. Z., Ruan, Y. & Cheng, F. MiR-363-3p promotes prostate cancer tumor progression by targeting Dickkopf 3. *J. Clin. Lab. Anal.* **36**, e24360. (2022).
18. Chang, J. et al. Mir-363-3p inhibits migration, invasion, and epithelial-mesenchymal transition by targeting NEDD9 and SOX4 in non-small-cell lung cancer. *J. Cell. Physiol.* **235**, 1808–1820 (2020).
19. Wang, K., Yan, L. & Lu, F. Mir-363-3p inhibits osteosarcoma cell proliferation and invasion via targeting SOX4. *Oncol. Res.* **27**, 157–163 (2019).
20. Rong, H. et al. Long non-coding RNA XIST expedites lung adenocarcinoma progression through upregulating MDM2 expression via binding to miR-363-3p. *Thorac. Cancer*. **11**, 659–671 (2020).
21. Brünner, N. et al. MCF7/LCC2: A 4-hydroxytamoxifen resistant human breast cancer variant that retains sensitivity to the steroidal antiestrogen ICI 182,780. *Cancer Res.* **53**, 3229–3232 (1993).
22. Burroughs, A. M., Kawano, M., Ando, Y., Daub, C. O. & Hayashizaki, Y. pre-miRNA profiles obtained through application of locked nucleic acids and deep sequencing reveals complex 5'/3' arm variation including concomitant cleavage and polyuridylation patterns. *Nucleic Acids Res.* **40**, 1424–1437 (2012).
23. Barzaman, K. et al. Breast cancer: Biology, biomarkers, and treatments. *Int. Immunopharmacol.* **84**, 106535 (2020).
24. Barchiesi, G. et al. Neoadjuvant endocrine therapy in breast Cancer: Current knowledge and future perspectives. *Int. J. Mol. Sci.* **21**. (2020).
25. Reinert, T. & Barrios, C. H. Optimal management of hormone receptor positive metastatic breast cancer in 2016. *Ther. Adv. Med. Oncol.* **7**, 304–320 (2015).
26. Droog, M., Beelen, K., Linn, S. & Zwart, W. Tamoxifen resistance: From bench to bedside. *Eur. J. Pharmacol.* **717**, 47–57 (2013).
27. Effects of chemotherapy and hormonal therapy for early breast cancer on recurrence and 15-year survival: An overview of the randomised trials. *Lancet (London England)* **365**, 1687–1717. (2005).
28. Nass, N. & Kalinski, T. Tamoxifen resistance: From cell culture experiments towards novel biomarkers. *Pathol. Res. Pract.* **211**, 189–197 (2015).
29. Ferragut Cardoso, A. P., Banerjee, M., Nail, A. N., Lykoudi, A. & States, J. C. miRNA dysregulation is an emerging modulator of genomic instability. *Semin Cancer Biol.* **76**, 120–131 (2021).
30. Li, Y. et al. Silencing long non-coding RNA HNF1A-AS1 inhibits growth and resistance to TAM of breast cancer cells via the microRNA-363/SERTAD3 axis. *J. Drug Target.* **29**, 742–753 (2021).
31. Liu, Y., Li, M., Yu, H. & Piao, H. lncRNA CYTOR promotes tamoxifen resistance in breast cancer cells via sponging miR–125a–5p. *Int. J. Mol. Med.* **45**, 497–509 (2020).
32. Khan, M. I. & Ahmad, A. LncRNA SNHG6 sponges miR-101 and induces tamoxifen resistance in breast cancer cells through induction of EMT. *Front. Oncol.* **12**, 1015428 (2022).
33. Soni, M. et al. O., and miR-489 confines uncontrolled Estrogen Signaling through a negative feedback mechanism and regulates tamoxifen resistance in breast Cancer. *Int. J. Mol. Sci.* **23**. (2022).
34. Shen, R. et al. MiRNA-155 mediates TAM resistance by modulating SOCS6-STAT3 signalling pathway in breast cancer. *Am. J. Translational Res.* **7**, 2115–2126 (2015).
35. He, M. et al. The miR-186-3p/EREG axis orchestrates tamoxifen resistance and aerobic glycolysis in breast cancer cells. *Oncogene* **38**, 5551–5565 (2019).
36. Ma, Y., Bu, D., Long, J., Chai, W. & Dong, J. LncRNA DSCAM-AS1 acts as a sponge of miR-137 to enhance tamoxifen resistance in breast cancer. *J. Cell. Physiol.* **234**, 2880–2894 (2019).
37. Dong, J., Geng, J. & Tan, W. MiR-363-3p suppresses tumor growth and metastasis of colorectal cancer via targeting SphK2. *Biomed. Pharmacother.* **105**, 922–931 (2018).
38. Downes, C. P. et al. Stimulation of PI 3-kinase signaling via inhibition of the tumor suppressor phosphatase, PTEN. *Adv. Enzyme Regul.* **47**, 184–194 (2007).
39. Li, A., Qiu, M., Zhou, H., Wang, T. & Guo, W. PTEN, insulin resistance and cancer. *Curr. Pharm. Des.* **23**, 3667–3676 (2017).
40. DiNitto, J. P., Cronin, T. C. & Lambright, D. G. Membrane recognition and targeting by lipid-binding domains. *Science's STKE: Signal Transduction Knowledge Environment* 2003, re16. (2003).
41. Stiles, B. et al. Essential role of AKT-1/protein kinase B alpha in PTEN-controlled tumorigenesis. *Mol. Cell. Biol.* **22**, 3842–3851 (2002).
42. Sen, A. et al. Assessments of prostate cancer cell functions highlight differences between a pan-PI3K/mTOR inhibitor, gedatolisib, and single-node inhibitors of the PI3K/AKT/mTOR pathway. *Mol Oncol* (2024).
43. Hakeem, A. N. et al. Piperine enhances doxorubicin sensitivity in triple-negative breast cancer by targeting the PI3K/Akt/mTOR pathway and cancer stem cells. *Sci. Rep.* **14**, 18181 (2024).
44. Majewska, A., Brodaczewska, K., Filipiak-Duliban, A., Kajdasz, A. & Kieda, C. miRNA Pattern in Hypoxic Microenvironment of Kidney Cancer-Role of PTEN. *Biomolecules* 12. (2022).

45. Dart, D. A., Uysal-Onganer, P. & Jiang, W. G. Prostate-specific PTen deletion in mice activates inflammatory microRNA expression pathways in the epithelium early in hyperplasia development. *Oncogenesis* **6**, 400 (2017).
46. Yuan, T. et al. Regulation of PI3K signaling in T-cell acute lymphoblastic leukemia: A novel PTEN/Ikaros/miR-26b mechanism reveals a critical targetable role for PIK3CD. *Leukemia* **31**, 2355–2364 (2017).
47. Costa, C. et al. PTEN loss mediates clinical cross-resistance to CDK4/6 and PI3Kα inhibitors in breast cancer. *Cancer Discov.*. **10**, 72–85 (2020).
48. Taha, M., Yousef, E., Badr, A. N., Salama, R. A. & Maurice, N. Expression profile and functional analysis of miR-301b in patients with breast cancer: A bioinformatics, biochemical, and histopathological study. *Pathol. Res. Pract.* **262**, 155536 (2024).

Author contributions
All authors contributed to the study conception and design. Yaning Liang, Cuiyu Shi, Wei Song and Rong Shen conducted experiments. Material preparation, data collection and analysis were performed by Yaning Liang, Cuiyu Shi, Yu Wang and Bingjie Fan. The first draft of the manuscript was written by Yaning Liang and Cuiyu Shi. Rong Shen supervised the work. All authors commented on previous versions of the manuscript. All authors read and approved the final manuscript.

Funding
This work was supported by the Natural Science Foundation of Shandong Province (ZR2020MH275).

Declarations

Competing interests
The authors declare no competing interests.

Ethics approval
This study was approved by the Ethics Committee of Shandong Provincial Hospital Affiliated to Shandong First Medical University (SMYX: NO. 2019-092).

Consent to participate
Not applicable.

Consent to publish
Not applicable.

Additional information
Correspondence and requests for materials should be addressed to R.S.